# Constraining the Marine Sr Budget from Natural Strontium Isotope Fractionation ($^{87}Sr/^{86}Sr^*/\delta^{88/86}Sr$) of Carbonates, Hydrothermal Solutions and River Waters

A. Krabbenhöft*, A. Eisenhauer*, F. Böhm*, H. Vollstaedt*, J. Fietzke*, V. Liebetrau*, N. Augustin*, B. Peucker-Ehrenbrink#, M. N. Müller*,[1], C. Horn*, B.T. Hansen°, N. Nolte° and K. Wallmann*

*Leibniz-Institut für Meereswissenschaften, IFM-GEOMAR, Wischhofstr. 1-3, 24148 Kiel, Germany

°Geowissenschaftliches Zentrum der Universität Göttingen (GZG), Abteilung für Isotopengeologie, Goldschmidtstr. 1, 37077 Göttingen, Germany

#Woods Hole Oceanographic Institution, Department of Marine Chemistry and Geochemistry, Woods Hole, Massachusetts, MA 02543, USA

Corresponding Author: A. Eisenhauer (aeisenhauer@ifm-geomar.de)

**Published in Geochimica et Cosmochimica Acta, 2010, 74: 4097–4109.**

## Abstract

Here we present Strontium (Sr) isotope values which, unlike traditional radiogenic $^{87}Sr/^{86}Sr$ measurements, are not normalized to a fixed $^{88}Sr/^{86}Sr$ ratio of 8.375209 (defined as $\delta^{88/86}Sr=0$ relative to NIST SRM 987). Instead isotope fractionation induced during mass-spectrometry measurement is corrected for using an $^{87}Sr/^{84}Sr$ double spike. This technique delivers two independent values for $^{87}Sr/^{86}Sr$ and $^{88}Sr/^{86}Sr$, respectively, reported as ($^{87}Sr/^{86}Sr^*/\delta^{88/86}Sr$). The difference between the traditional radiogenic ($^{87}Sr/^{86}Sr/\delta^{88/86}Sr=0$) and the new ($^{87}Sr/^{86}Sr^*/\delta^{88/86}Sr$)-values reflect natural mass-dependent isotope fractionation. In order to constrain glacial/interglacial changes of the marine Sr budget we compare the isotope composition of modern seawater ($(^{87}Sr/^{86}Sr^*/\delta^{88/86}Sr)_{Seawater}$) and of modern marine biogenic carbonates ($(^{87}Sr/^{86}Sr^*/\delta^{88/86}Sr)_{Carbonates}$) with the corresponding values of river waters ($(^{87}Sr/^{86}Sr^*/\delta^{88/86}Sr)_{River}$) and hydrothermal solutions ($(^{87}Sr/^{86}Sr^*/\delta^{88/86}Sr)_{HydEnd}$) in a three-isotope-plot. The measured $(^{87}Sr/^{86}Sr^*/\delta^{88/86}Sr)_{River}$-values of selected rivers reflect ~18 % of the global Sr discharge and correspond to a Sr flux weighted mean of (0.7114(8)/0.315(8) ‰). The $(^{87}Sr/^{86}Sr^*/\delta^{88/86}Sr)_{HydEnd}$-value averaging hydrothermal solutions from the Atlantic Ocean are determined to be (0.7045(5)/0.27(1) ‰). In contrast the $(^{87}Sr/^{86}Sr^*/\delta^{88/86}Sr)_{Carbonates}$-values representing the marine Sr output are (0.70926(2)/0.21(2) ‰). The isotope difference between calculated Sr isotope input (0.7104(8)/0.310(8) ‰) and output values are interpreted as to reflect isotope disequilibrium concerning Sr input and output. In contrast a glacial low sea level-stand scenario taking into a account a ten times higher supply of Sr from shelf carbonate weathering relative to the modern input indicates isotope equilibrium between input and output values at these times.

---

[1] Present address: Laboratoire d'Océanographie de Villefranche-sur-Mer, UMR 7093, Station Zoologique, BP 28, 06234 Villefranche-sur-mer, France

## 1. Introduction

The radiogenic Sr isotope composition ($^{87}Sr/^{86}Sr$: ~0.709175, (VEIZER, 1989)) is homogeneously distributed in the oceans and equal to the isotopic composition of modern marine carbonates (FAURE and FELDER, 1981; MCARTHUR, 1994; MCARTHUR et al., 2001). This is due to the long Sr residence time of 2.4 Ma compared to the mixing time of the oceans in the order of ~1.5 ka. The modern $^{87}Sr/^{86}Sr$ ratio of ocean waters is mainly generated by mixing of two isotopically distinct sources 1) Sr from the weathering of old rubidium (Rb)-rich continental silicate rocks that have been enriched in $^{87}Sr$ by the decay of $^{87}Rb$; 2) Sr with a low $^{87}Sr/^{86}Sr$ ratio derived from the Earth´s mantle, which is mainly released into the ocean by the reaction of seawater circulating through ocean crust at mid-ocean ridges and ridge flanks (GODDERIS and VEIZER, 2000; PALMER and EDMOND, 1992). A minor Sr influx from diagenetic alteration and dissolution of sediments on the ocean floors has an intermediate $^{87}Sr/^{86}Sr$ value close to that of seawater (ELDERFIELD and GIESKES, 1982).

While riverine $^{87}Sr/^{86}Sr$ ratios are distinctly different from seawater values the large difference in Sr concentration ($[Sr]_{Rivers}$~1.0 µM, $[Sr]_{Seawater}$~90 µM) ensures that even in marginal seas with high riverine input, seawater $^{87}Sr/^{86}Sr$ values are close to the normal marine value ($^{87}Sr/^{86}Sr$=0.709175). Exceptions are brackish seas such as the Baltic Sea with salinities below 15 psu (ANDERSSON et al., 1992). The average Sr concentration in river waters dominated by silicate weathering input is 0.2 µM, and the average $^{87}Sr/^{86}Sr$ ratio is 0.705 for young magmatic provinces and 0.735 for old crustal segments (PALMER and EDMOND, 1992). Rivers draining carbonate rocks, in contrast, have much higher Sr concentrations of ~4 µM, while $^{87}Sr/^{86}Sr$ ratios are ranging from 0.707 to 0.709 (GAILLARDET et al., 1999). This results in an average global river water Sr concentration of about 1 µM and a $^{87}Sr/^{86}Sr$ ratio of 0.7119 (GAILLARDET et al., 1999). About one third of this riverine Sr is derived from silicate weathering and about two thirds from carbonate weathering (GAILLARDET et al., 1999; PALMER and EDMOND, 1989)

Although the principal mechanisms of marine Sr geochemistry are well understood there is an ongoing discussion (c.f. (VANCE et al., 2009) about the influence of glacial/interglacial changes of weathered continental material on the marine Sr budget on glacial/interglacial time scales. Recent findings indicate that ~70% of the silicate weathering flux is affected by non-steady-state processes, possibly creating a ~100 ka periodicity and an imbalance between input and output fluxes over the Quaternary (VANCE et al., 2009). However, the Sr imbalance created by the non-steady state conditions cannot be quantified by the radiogenic Sr ratios alone. Marine Sr budget calculations based on the radiogenic Sr focus on the input fluxes only because marine calcium carbonate ($CaCO_3$) and seawater show identical radiogenic Sr isotope values. This is a direct consequence of the normalization of the measured $^{87}Sr/^{86}Sr$ ratio to a fixed $^{88}Sr/^{86}Sr$ ratio of 8.375209 (NIER 1938) to correct for mass

dependent isotope fractionation in nature and during mass-spectrometer measurement, thereby any information about natural isotope fractionation is lost.

In order to overcome these problems inherent to the radiogenic Sr system we determined the values of stable Sr isotope fractionation applying the TIMS double spike technique (KRABBENHÖFT et al., 2009). First results showed that $\delta^{88/86}Sr_{Seawater}$ is different from NIST SRM987 showing a ratio of 0.38(1) ‰ and is homogeneously distributed in the oceans (LIEBETRAU et al., 2009). Furthermore, it was shown that the Sr isotope composition of marine carbonates ($\delta^{88/86}Sr_{Carbonates}$) like corals is ~0.2 ‰ lighter than $\delta^{88/86}Sr_{Seawater}$ due to isotope fractionation during $CaCO_3$ precipitation (FIETZKE and EISENHAUER, 2006; HALICZ et al., 2008; OHNO et al., 2008). Measurements of (HALICZ et al., 2008; OHNO et al., 2008) showed that marine basalt has a $\delta^{88/86}Sr$ of ~0.25 ‰ which is different from continental igneous rocks and soils that show lighter values in the range of ~ -0.2 to 0.2 ‰ for rhyolites and granites respectively. However, due to its novelty the $\delta^{88/86}Sr$ database is still very limited pending future measurements and confirmations.

Taking natural Sr isotope fractionation into account the Sr isotope composition for marine $CaCO_3$ and seawater are different allowing the simultaneous calculation of input as well as of output flux values from Sr budget equations. This new approach completes and extends the well established radiogenic Sr isotope systematic with an additional dimension and allows the simultaneous measurement of paired ($^{87}Sr/^{86}Sr^*/\delta^{88/86}Sr$) ratios (see Appendix 1 for definition and notation). In this regard the most important advantage of measuring paired ($^{87}Sr/^{86}Sr^*/\delta^{88/86}Sr$) values is that a complete isotope balance of the oceans Sr budget can now be calculated.

Here we present first results of paired ($^{87}Sr/^{86}Sr^*/\delta^{88/86}Sr$) ratios of rivers, hydrothermal fluids, marine carbonates and seawater in order to constrain the status of the modern marine Sr budget.

## 2. Materials and Methods

### 2.1 River Waters

In order to reevaluate the Sr isotope supply via river discharge to the ocean and to constrain the riverine Sr-budget for paired ($^{87}Sr/^{86}Sr^*/\delta^{88/86}Sr$) ratios, a suite of rivers representing ~18 % of the global annual riverine Sr flux to the ocean was sampled for measuring their ($^{87}Sr/^{86}Sr^*/\delta^{88/86}Sr$) composition. The Sr isotope values are presented together with additional information about the river water discharge, sampling locations and the riverine Sr-fluxes in Tab. 1 and Fig. 1. The analyzed rivers drain various proportions of 9 of the 16 large scale exoreic drainage regions on earth (GRAHAM et al., 1999; PEUCKER-EHRENBRINK and MILLER, 2004). Assuming the river water samples of this study to be representative for the 9 large-scale draining regions, both the average bedrock age (399 Ma) and the relative abundances of sedimentary (70%), volcanic (9%) and intrusive/metamorphic (21%) bedrock are similar to

that of global exoreic bedrock weighted according to water discharge (405 Ma, 73%, 9%, 18%, respectively). The set of rivers thus does not appear to be significantly biased with respect to the lithological setting and age of the bedrock (PEUCKER-EHRENBRINK and MILLER, 2004).

### 2.2 Hydrothermal solutions

Under low temperature conditions the net effect of hydrothermal circulation is an enrichment of Sr in the fluid (BUTTERFIELD et al., 2001; MOTTL et al., 1998). This effect has also been found at high-temperature vent sites where the Sr concentrations of hydrothermal waters originating from mid-ocean ridge vents have been measured at the East Pacific Rise and Iceland to be about ~130(60) µM with a $^{87}Sr/^{86}Sr$ ratio of ~0.7035(5) (VEIZER, 1989) and to range from 44 to 156 µM with $^{87}Sr/^{86}Sr$ ratios ranging from 0.7037(1) to 0.7045(1) for different vents (RAVIZZA et al., 2001). Similar values were measured at the Logatchev hydrothermal field indicating a $[Sr]_{HydEnd}$ concentration of ~125(5) µM and a $^{87}Sr/^{86}Sr$ ratio of 0.7034(4) (AMINI et al., 2008).

Seven hydrothermal vent-fluid samples from the active 4°48´S area on the Mid-Atlantic Ridge (MAR) were analyzed for this study (Tab. 2). The 4°48´S hydrothermal system is situated on-axis at the MAR at water depths around 3000 m. It is dominated by slightly altered to fresh lava flows and pillows (HAASE et al., 2007). On this plateau at least three high-temperature vent fields (Turtle Pits [TP], Comfortless Cove [CC] and Red Lion [RL]) are situated on a flat, volcanically and tectonically active 2 km wide section (HAASE et al., 2007). The samples analyzed in this study were taken from these high-temperature vent fields using ROV techniques with a “Multiport Valve-based all-Teflon Fluid sampling system, (KIPS)” during the RV l´Atalante cruise MARSUED IV in 2007. Comfortless Cove as well as TP are characterized by high fluid-temperatures >407 °C at 2990 m water depth, close to the critical point of seawater showing indications of phase separation (HAASE et al., 2007). The RL vent field emits fluids at ~370°C that show no indications of phase separation.

The measured Mg and Sr concentrations of the fluids are positively correlated suggesting that $[Sr]_{HydEnd}$ is lower than in seawater. From the extrapolated Mg/Sr ratios of the TP and CC fluid samples to a Mg/Sr ratio of zero, a $[Sr]_{HydEnd}$ of 34(5) µM is computed. Likewise, the $[Sr]_{HydEnd}$ of RL was extrapolated to be ~56(5) µM. Sr isotope compositions measured throughout this study are presented in Tab. 2 and in Fig. 2a and b.

### 2.3 Marine carbonates

The major sink for Sr in the ocean is the sedimentation of aragonitic and calcitic $CaCO_3$ (MILLIMAN and DROXLER, 1996) where calcium (Ca) is substituted by Sr. In order to quantify the Sr burial flux and its isotope composition we performed Sr isotope measurements on the major marine calcifying organisms which are summarized together with other related information in Tab. 3. It can be seen that the $CaCO_3$ deposition rate is almost equally

distributed between reef corals, coccoliths and planktic foraminifera although the largest contribution comes from those species (e.g mussels, star fish, sea urchins, benthic foraminifera, bryozoa, calcareous algae, etc.) living on the shelves and slopes (~49 %). The higher Sr concentration of aragonite is expressed by relatively larger Sr/Ca ratios than in calcite (see Tab. 3). The Sr/Ca ratios are well constrained for reef corals, Halimeda, planktic foraminifera and also for many shelf and slope species (e.g. mussels: 1.5 mmol/mol, star fish: 2.5 mmol/mol, aragonitic algae: ~10 mmol/mol). However, the average value cannot be well constrained for the generalized shelf and slope species because the relative distribution of calcite and aragonite on the shelves is not well known and may vary from 1.4 (calcitic mussels) up to >11 mmol/mol (aragonitic algae). For further discussion we arbitrarily assume the shelf species to be two-third aragonitic (Sr/Ca ~9 mmol/mol) and one-third calcitic (Sr/Ca ~1.8 mmol/mol) approaching an average shelf carbonate Sr/Ca ratio of ~6.6 mmol/mol. The global average isotope values for shelf carbonates then amounts to (0.70924(1)/0.22(3) ‰).

**2.4 Sample preparation**

All solid carbonate samples were weighed in Teflon beakers together with 2 ml $H_2O$ (18.2 MΩ Milli-Q water). About 500 µl 4.5 N $HNO_3$ was added in order to dissolve the samples. Samples were heated for at least 5 hours and dried at ~90 °C. In order to remove organic substances 50 µl $H_2O_2$ were added together with 200 µl 2N $HNO_3$ and samples were heated up to ~80 °C for at least 5 hours in closed beakers. Following this procedure samples were dried again at ~80°C, dissolved with 2 ml 8 N $HNO_3$ and splitted into two fractions. The fractions each contained 1000 – 1500 ng Sr, corresponding to a carbonate sample weight of 1 to 2 mg. The Sr double spike was added to one fraction. Both fractions were dried again at ~90 °C. Chromatographic column separation was performed using BIO-RAD 650 µl columns filled to 1/3 with Eichrom Sr-SPS resin (grain size 50-100µm). The resin was washed 3 times with 4.5 ml $H_2O$ and 4.5 ml 8N $HNO_3$. After cleaning the resin was conditioned with 3x1 ml 8N $HNO_3$. The sample was loaded onto the column dissolved in 1 ml 8N $HNO_3$. In order to remove the sample matrix the resin was washed with 6x1 ml 8N $HNO_3$. The remaining Sr-fraction was eluted by 3x1 ml $H_2O$ into a Teflon beaker. To remove potentially washed-out residual resin the elutes were dried down and heated up to 80°C in 50 µl $H_2O_2$ and 200 µl 2N $HNO_3$ at 80 °C for at least 5 hours in closed beakers. Finally samples were dried at ~80 °C. About 500 ng Sr was loaded together with 2 µl $H_3PO_4$ onto a Re single filament after 1.5 µl of $Ta_2O_5$-activator was added in order to stabilize signal intensity. The sample is then heated at 0.6 A to near dryness on the filament. The sample was dried at 1 A and slowly heated up to 1.8 A within 2 minutes. Finally the sample was heated up until a dark red glow was visible. After keeping the filament glowing for about 30 seconds the current was turned down and the filament was mounted onto the sample wheel. Beside the dissolving step the hydrothermal- and river water samples were treated in the same way as described above.

### 2.5 TIMS measurement procedure

The application of an $^{87}Sr/^{84}Sr$ double spike allows the determination of natural Sr fractionation due to the correction for mass-dependent fractionation during the course of the TIMS measurements. The details of the $^{87}Sr/^{84}Sr$ double spike production, measurement procedure and data reduction are given in (KRABBENHÖFT et al., 2009).

Our Sr isotope measurements were carried out at the IFM-GEOMAR mass spectrometer facilities in Kiel and at the "Geowissenschaftliches Zentrum der Universität Göttingen", Germany. At both locations we used TRITON mass spectrometers (ThermoFisher, Bremen, Germany) which operate in positive ionization mode with a 10 kV acceleration voltage and a $10^{11}$ Ω resistor for the Faraday cups. The instruments are equipped with nine moveable Faraday cups as detection system which account for the dispersion of the entire Sr isotope mass range from ~84 to 88 amu, respectively.

Mass 85 was measured in order to monitor the interfering $^{87}Rb$ assuming an $^{85}Rb/^{87}Rb$ ratio of 2.59. Data were acquired at a typical signal intensity of 10 V on mass 88, with an average filament temperature of about 1450°C. For each sample 9 blocks with 14 cycles corresponding to 126 single scans are measured. Before each block the baseline was recorded and the amplifier rotation was performed.

For applying the $^{87}Sr/^{84}Sr$ double spike technique, two separate analyses for each sample are necessary: one ic-analysis (ic = isotope composition; unspiked) and one id-analysis (id = isotope dilution; spiked) where the $^{86}Sr/^{84}Sr$-, $^{87}Sr/^{84}Sr$- and $^{88}Sr/^{84}Sr$-ratios of the double spike are well known. The $^{86}Sr/^{84}Sr$- and the $^{88}Sr/^{84}Sr$-ratios are normalized to the mean of the first block of the $^{87}Sr/^{84}Sr$ isotope ratio using an exponential fractionation law in an offline data processing after the TIMS measurement. Following this procedure the average internal precision of the single measurements is ~7 ppm (RSD) for the $^{86}Sr/^{84}Sr$-ratio and ~9 ppm for the $^{88}Sr/^{84}Sr$-ratio in the ic-analyses. We measured ~11 ppm (RSD) for the $^{86}Sr/^{84}Sr$-ratio and ~21 ppm for the $^{88}Sr/^{84}Sr$-ratio in the id-analyses. Variations of the $^{88}Sr/^{86}Sr$ are reported in the usual δ-notation: $\delta^{88/86}Sr\ [‰]=(^{88}Sr/^{86}Sr_{sample}/^{88}Sr/^{86}Sr_{SRM987}-1)*1000$. For normalization the SRM987 standard has been chosen having an internationally accepted value for $^{88}Sr/^{86}Sr$ of 8.375209 (NIER 1938).

For the use of notations (e.g. $^{87}Sr/^{86}Sr_{Norm}$ and $^{87}Sr/^{86}Sr^*$) and additional information about mass-dependent fractionation we refer to Appendix 1.

## 3. Results

### 3.1 Sr isotope composition of the marine input

#### 3.1.1 Sr composition of the riverine discharge to the ocean

Concerning the rivers presented in Tab. 1 and Fig. 1 the $^{87}Sr/^{86}Sr_{Norm}$ and $^{87}Sr/^{86}Sr^*$ show variations from 0.707321(8) to 0.727705(9) and from 0.707417(9) to 0.727798(6), respectively. The Sr flux weighted mean river value for $^{87}Sr/^{86}Sr_{Norm}$ and $^{87}Sr/^{86}Sr^*$ amounts to

0.7113(4) and 0.7114(8), respectively. In particular the $^{87}Sr/^{86}Sr_{Norm}$ –value is in good accordance with the value published by (GAILLARDET et al., 1999). The $\delta^{88/86}Sr$ values vary in between 0.243(6) ‰ for the Lena river and 0.42(2) ‰ for the Maipo river. The Sr flux weighted mean ($^{87}Sr/^{86}Sr^*/\delta^{88/86}Sr$) value is (0.7114(8)/0.315(8) ‰). Note the good agreement of the $^{87}Sr/^{86}Sr_{Norm}$ values with the conventional $^{87}Sr/^{86}Sr$ values in Tab. 1. This clearly indicates that the applied double spike method can reproduce conventional radiogenic values in addition to the new information on the natural Sr isotope composition of the measured samples.

### 3.1.2 Sr isotope composition of the hydrothermal discharge to the ocean

Following the procedure of (AMINI et al., 2008) and assuming that the pure hydrothermal solution is free of Mg we estimate the $(^{87}Sr/^{86}Sr^*/\delta^{88/86}Sr)_{HydEnd}$-values to be (0.7045(5)/0.27(1) ‰) for a seawater free hydrothermal end member fluid by extrapolating the measured values to an Mg/Sr ratio of zero (Tab. 2, Fig. 2a, b).

Note, that the $\delta^{88/86}Sr_{HydEnd}$ values are isotopically lighter than seawater. This is in good agreement with the reported radiogenic $^{87}Sr/^{86}Sr$- and $\delta^{88/86}Sr$-value of basalt of 0.70412(4) and 0.26(3) ‰, respectively (OHNO et al., (2008)). Latter observation indicates that the isotopic composition of the hydrothermal fluids mainly represents the isotopic composition of the ocean crust.

### 3.1.3 Sr composition of the combined riverine and hydrothermal input to the ocean

From the measured and compiled values of the riverine discharge and of the hydrothermal input a mean ocean input flux and its corresponding isotope composition can be estimated (Tab. 4) ($(^{87}Sr/^{86}Sr^*/\delta^{88/86}Sr)_{Input}$: ~0.7104(8)/~0.310(8) ‰). Latter values are certainly burdened with larger uncertainties because the calculation is based on several assumptions as described in Tab. 4. The calculated isotope values show that the present day Sr supply is mainly (~60 %) controlled by Sr delivered by riverine discharge to the ocean. From the data compilation in Tab. 4 an input flux of about $\sim 56 \cdot 10^9$ mol/a can be estimated. Latter flux is in good agreement with the flux estimated by (STOLL and SCHRAG, 1998) and (STOLL et al., 1999) to be $\sim 40 \cdot 10^9$ mol/a.

### 3.2 Isotope composition of the marine Sr output

The primary sink for marine Sr is dominated by the Sr burial flux due to marine carbonate precipitation. In order to determine the average isotope composition we determined the available paired $^{87}Sr/^{86}Sr^*/\delta^{88/86}Sr$ values for tropical corals, green algae, foraminifera and coccoliths presented in Tab. 3. These species are considered to be the most important carbonate producing taxa in the modern oceans.

For corals we adopted the ($^{87}Sr/^{86}Sr^*/\delta^{88/86}Sr$)-value of the JCp-1 coral standard (0.70923(8)/0.19(1) ‰). Aragonitic azooxanthellate cold water corals of the species *Lophelia*

*pertusa* that grew between 6 and 10°C show slightly lower $\delta^{88/86}Sr$ values, ranging from 0.13 to 0.18 ‰ (RÜGGEBERG et al., 2008). However, cold water corals contribute only ~1 % to the global carbonate sediment budget (LINDBERG and MIENERT, 2005) and are therefore not considered in the Sr isotope budget. In contrast tropical coral reefs contribute about 31 % to the ocean´s Sr burial flux (Tab. 3). Concerning tropical corals we did not take any temperature sensitivity of the paired ($^{87}Sr/^{86}Sr^*/\delta^{88/86}Sr$)-values previously predicted by (FIETZKE and EISENHAUER, 2006) into account. This is because measurements of higher precision by the application of our new double spike technique failed to confirm the earlier predicted temperature sensitivity of Sr isotope fractionation.

For this study paired ($^{87}Sr/^{86}Sr^*/\delta^{88/86}Sr$)-values of aragonitic Halimeda specimen from Tahiti and the Mediterranean Sea were measured showing average values of 0.70926(3)/0.27(3) ‰ (Tab. 3). Halimeda mounds contribute ~9 % to the ocean´s Sr burial flux.

Although being calcitic the ($^{87}Sr/^{86}Sr^*/\delta^{88/86}Sr$)-values of ~0.70926(3)/0.26(7) ‰ from cultured coccoliths are similar to the values of the aragonitic species (Tab. 3). Coccoliths contribute ~6 % to the global Sr burial flux.

The two species *G. ruber* and *G. sacculifer* are taken to be representative for the Sr isotope composition of calcitic planktic foraminifera. They show identical ($^{87}Sr/^{86}Sr^*/\delta^{88/86}Sr$)-values of (0.70920(2)/0.14(1) ‰). Note, that the paired ($^{87}Sr/^{86}Sr^*/\delta^{88/86}Sr$)-values value of these foraminifera are considerably lower than for the other species pointing to a strong physiological control on the trace metal uptake in planktic foraminifera. Similar to the coccoliths planktic foraminifera contribute ~5 % to the ocean´s Sr burial flux.

A significant part of the Sr flux is contributed by non reefal carbonate production on the continental shelf and slope species like mussels, starfish and others (MILLIMAN and DROXLER, 1996). However, the shelf carbonate contribution is burdened with large uncertainty due to the unknown partitioning between calcitic and aragonitic species and the lag of knowledge on the precise $CaCO_3$ production rates of different contributing taxa (see Tab. 3). Based on the data compiled in Tab. 3 and in a first order approach we calculated the mean ($^{87}Sr/^{86}Sr^*/\delta^{88/86}Sr$)-ratios for the shelf carbonates to be ~(0.70924(1)/0.22(3) ‰) assuming the shelf and slope carbonates to be two-third aragonitic (mean ($^{87}Sr/^{86}Sr^*/\delta^{88/86}Sr$) of reef corals and Halimeda: (0.70925/0.23 ‰) and one-third calcitic (mean ($^{87}Sr/^{86}Sr^*/\delta^{88/86}Sr$) of coccoliths and planktic foraminifera: 0.70923/0.20 ‰).

Summarizing the data of Tab. 3 we can calculate the flux weighted $^{87}Sr/^{86}Sr^*/\delta^{88/86}Sr$-ratios of the total marine carbonate production to be (~0.70926(2)/~0.21(2) ‰). Latter Sr isotope values are taken to represent the Sr output values for further budget calculations.

## 4. Discussion

The preliminary compilations of the input and output data in Tab. 4 shows that the Sr output flux (~$174 \cdot 10^9$ mol/a) is obviously significantly larger than the Sr input (~$56 \cdot 10^9$ mol/a) and

that the Sr isotope compositions of input and output are considerably different both indicating that $[Sr]_{Seawater}$ is decreasing and that the equilibrium between input and output must have been disturbed by distinct geological processes in the past. In order to examine this observation in more detail we may compare the Sr isotope balance of input, output and of seawater in a three-isotope-plot. This approach is new in Sr isotope geochemistry and can only be done by taking Sr isotope fractionation into account.

**4.1 Sr budget of the global ocean**

In Fig. 3 the flux weighted mean of the $(^{87}Sr/^{86}Sr^*/\delta^{88/86}Sr)_{River}$- and $(^{87}Sr/^{86}Sr^*/\delta^{88/86}Sr)_{HydroEnd}$-values are the two end-members of a binary mixing line between the two major sources for Sr in the modern ocean. The joined $(^{87}Sr/^{86}Sr^*/\delta^{88/86}Sr)_{Input}$-value of hydrothermal and riverine input fall along the binary mixing line and plot relatively close to the Sr isotope composition of the average rivers indicating that riverine input is the major source for Sr (~60 %) today.

In contrast, the modern Sr isotope values of $(^{87}Sr/^{86}Sr^*/\delta^{88/86}Sr)_{Seawater}$ and of $(^{87}Sr/^{86}Sr^*/\delta^{88/86}Sr)_{Carbonates}$ form a mass-dependent Sr isotope fractionation line. Marine carbonates are isotopically lighter than seawater because precipitation of carbonates prefers the lighter isotopes and leave the seawater enriched in the heavy Sr isotopes. The intercept of the binary mixing line and the fractionation line ($(^{87}Sr/^{86}Sr^*/\delta^{88/86}Sr)_{Intercept}$. (~0.70927(1)/~0.30(2) ‰) is actually defining the isotope composition of the Sr input into the ocean. However, intercept and calculated input values are significantly different indicating that there is isotope disequilibrium in the Sr budget. The discrepancy between the calculated $(^{87}Sr/^{86}Sr^*/\delta^{88/86}Sr)_{Input}$-value and the $(^{87}Sr/^{86}Sr^*/\delta^{88/86}Sr)_{Intercept}$-value can be calculated to be in the order of (~0.0011(8)/~0.01(2)‰). Latter discrepancy indicate that the combined riverine and groundwater input (~$49.3 \cdot 10^9$ mol/a) is by about a factor of two or taken only the rivers into account a factor of four too high in order to be in equilibrium with the calculated intercept value. This observation is in general accord with earlier statements that the riverine flux obtained from observations of modern rivers is broadly accurate, but not representative of timescales appropriate for elements with oceanic residence longer than Quaternary glacial/interglacial cycles and that weathering rates remain about two to three times the average for an entire late Quaternary glacial cycle (VANCE et al., 2009). Following earlier arguments (c.f. BLUM and EREL, 1995) that chemical weathering rates on modern Earth are likely to remain far from equilibrium owing to the physical production of finely ground material at glacial terminations that acts as a fertile substrate for chemical weathering creating a pulse of rapid chemical weathering. This pulse has yet not decayed away and remains about two to three times the average for an entire late Quaternary glacial cycle (VANCE et al., 2009).

There is also a significant difference between the Sr isotopic composition of the $(^{87}Sr/^{86}Sr^*/\delta^{88/86}Sr)_{Input}$ –value and the output value represented by $(^{87}Sr/^{86}Sr^*/\delta^{88/86}Sr)_{Carbonates}$ of (~0.0011(8)/~0.10(2)‰). In Sr isotope equilibrium it is supposed that the $(^{87}Sr/^{86}Sr^*/\delta^{88/86}Sr)_{Input}$ equals $(^{87}Sr/^{86}Sr^*/\delta^{88/86}Sr)_{Carbonates}$ and that the elemental fluxes in and

out of the ocean are identical. Hence, our observations indicate an isotope disequilibrium concerning Sr input and output fluxes in the modern ocean (see Appendix 4).

In order to reconcile these observations we have to assume that a past isotope equilibrium must have been disturbed due to a differential change of the Sr input and output flux, respectively. Disturbances of pre-existing isotope equilibria can be observed when additional Sr contributions are sufficiently large (STOLL and SCHRAG, 1998) relative to the amount of Sr in the ocean and when the related isotope composition is significantly different to the one of seawater. Furthermore, any Sr isotope disequilibrium in the ocean will persist only for a time interval compatible to its residence time of ~2.4 Ma in the ocean. Processes which occur on much longer time scales may change in equilibrium not causing any disequilibrium between input and output fluxes. Following this approach it is very unlikely that the fluxes and Sr isotope composition of hydrothermal fluids are subject to a rapid change. This is because mid ocean ridge hydrothermal circulation is controlled by processes in the Earth´s mantle which occur on multi-million year timescales exceeding the residence time of Sr in the marine ocean to a large extend.

Changes of the preferred carbonate polymorphism may also lead to a change in Sr concentration of seawater due to the approximately one order of magnitude higher Sr/Ca ratio of aragonite in contrast to calcite. Measurements of calcitic foraminifera (Tab. 3) indicate different fractionation factors between aragonite and calcite like it is already known from Ca isotope measurements (FARKAŝ et al., 2007). This could lead to changes in the isotopic composition of seawater. However, similar to hydrothermal processes global changes of the preferred marine carbonate polymorphism occur on time scales much longer than the Sr residence time (STANLEY and HARDIE, 1998). In contrast, riverine input into the ocean may be subject of relatively rapid changes when compared to the Sr residence time and can occur on glacial/interglacial time scales in the order of ~100 ka. In addition, the related glacial/interglacial sea level changes and the consequent exposure of continental shelves composed to a large extend of carbonates may be responsible for the disturbance of the Sr isotope equilibrium between input and output of the ocean (STOLL and SCHRAG, 1998).

**5. Sr imbalance in the ocean on glacial/interglacial time scales**

Beside other factors a sealevel drop in the order of ~120 m (c.f. FAIRBANKS, 1989) will cause an exposure of the continental shelves providing an additional supply of elements from the continents to the ocean. In particular alkaline earth elements like Mg, Ca and Sr will be supplied from carbonate dominated continental shelves in higher amounts during the glacials than during interglacials. In regard of the elements Mg and Sr the polymorphisms is a major controlling factor because calcite contains relative more Mg than aragonite whereas aragonite contains about 10 times more Sr than calcite (Tab. 3). Aragonite will eventually recrystalize to calcite during meteoric diagenesis and release Sr to the sea. As demonstrated by (STOLL and SCHRAG, 1998) and (STOLL et al., 1999) during glaciations associated with

sea level lowstands the ocean is increasing its Sr/Ca ratio due to an additional contribution of Sr from continental shelf weathering. In contrast during interglacials the shelves act as a Sr sink causing the seawater Sr/Ca ratio to decrease. These glacial to interglacial variations results in an oscillation of the Sr/Ca ratio in the order of about ±1 % relative to the present day value (STOLL and SCHRAG, 1998).

From the integration of the (STOLL and SCHRAG, 1998) data one can estimate the average annual Sr flux to the ocean in the time interval from 10 to 20 ka before present is in the order of ~$150 \cdot 10^9$ mol/a which is about a factor of ~3 larger than the compilation of modern Sr fluxes supplied by continental discharge and hydrothermal activity (~$56 \cdot 10^9$ mol/a, Tab. 4). As a consequence during the last glacial maximum the Sr input was dominated by continental carbonate shelf weathering rather than by the weathering of continental silicates. Taking shelf carbonate weathering into account and adopting the values given by (STOLL and SCHRAG, 1998) we can estimate a glacial ($^{87}Sr/^{86}Sr^*/\delta^{88/86}Sr)_{Input}$-value of (~0.7096/~0.24 ‰) being considerably lower than the present day ($^{87}Sr/^{86}Sr^*/\delta^{88/86}Sr)_{Input}$-value of (0.7104(8)/0.310(8) ‰). In particular the estimated glacial ($^{87}Sr/^{86}Sr^*/\delta^{88/86}Sr)_{Input}$-values are within uncertainty relative close to the modern ($^{87}Sr/^{86}Sr^*/\delta^{88/86}Sr)_{Carbonates}$-values of (0.70926(2)/0.21(2) ‰) indicating isotope equilibrium rather disequilibrium conditions during the last glacial maximum (Fig. 3).

## 6. Conclusion

Instead of having two sources supplying Sr to the ocean as today three major Sr sources were active during the last glacial: riverine Sr, hydrothermal Sr input (0.7104(8)/0.310(8) ‰) and weathering of continental shelf carbonates with a combined glacial Sr isotopic composition in the order of (~0.70926/~0.21 ‰). In addition, silicate weathering of Sr and supplied by the rivers must have been considerably lower in the glacial. Most likely, the Sr isotope system was close or in isotope equilibrium during the last glacial. However, the glacial Sr equilibrium were driven to modern ocean Sr disequilibrium because the weathering regime changed drastically due to the relatively rapid post glacial sea level rise terminating continental shelf exposure and emphasizing riverine and more silicate dominated Sr fluxes at the last glacial/interglacial transition. In particular, the riverine input of Sr via riverine input increased drastically due to the fine grained material which remained after the wanning of the glacial ice masses as a fertile substrate for chemical weathering. Latter peak is still not decayed away as seen from our data. As a consequence of the relative long Sr residence time of ~2.4 Ma relative to the 100 ka periodicity of glacial/interglacial variations the difference in the isotope composition of the Sr output an input still reflect glacial conditions and have yet not relaxed to the post-glacial and modern weathering conditions.

**Acknowledgements**

Financial support was provided by the “Deutsche Forschungsgemeinschaft, DFG” Ei272/29-1 and Ei272/30-1 (TRION). Mrs. A. Kolevica is acknowledged for laboratory assistance and technical support. The comments and suggestions of two anonymous reviewer helped to significantly improve this publication. The help of the associate editor Prof. S. Krishnaswami is gratefully acknowledged.

**References:**


Amini, M., Eisenhauer, A., Böhm, F., Fietzke, J., Bach, W., Garbe-Schönberg, D., Rosner, M., Bock, B., Lackschewitz, K. S., and Hauff, F., 2008. Calcium Isotope ($\delta^{44/40}$Ca) Fractionation Along Hydrothermal Pathways, Logatchev Field (Mid-Atlantic Ridge, 14° 45'N). *Geochim. Cosmochim. Acta* 72, 4107-4122.

Andersson, P. S., Wasserburg, G. J., and Ingri, J., 1992. The Sources and Trasport of Sr and Nd Isotopes in the Baltic Sea. *Earth Planet. Sci. Lett.* 113, 459-472.

Basu, A. R., Jacobsen, S. B., Poreda, R. J., Dowling, C. B., and Aggarwal, P. K., 2001. Large Groundwater Strontium flux to the Oceans from the Bengal Basin and the Marine Strontium Isotope Record. *Science* 293, 1470-1473.

Blum and Erel, 1995. A silicate weathering mechanism linking increases in marine 87Sr/86Sr with global glaciation. Nature, 373, 415-418.

Broecker, W. and Clark, E., 2009. Ratio of coccolith $CaCO_3$ to foraminifera $CaCO_3$ in late Holocene deep sea sediments. *Paleoceanography* 24, doi:10.1029/2009PA001731.

Butterfield, D. A., Nelson, B. K., Wheat, C. G., Mottl, M. J., and Roe, K. K., 2001. Evidence for Basaltic Sr in Mid Ocean Ridge-Flank Hydrothermal Systems and Implications for the Global Oceanic Sr Isotope Balance. *Geochim. Cosmochim. Acta* 65, 4141-4153.

Cohen, A. L. and Thorrold, S. R., 2007. Recovery of Temperature Records from slow-growing Corals by fine Scale Sampling of Skeletons. *Geophys. Res. Lett.* 34, 6, L17706, doi:10.1029/2007GI030967.

Davis, A. C., Bickle, M. J., and Teagle, D. A. H., 2003. Imbalance in the Oceanic Strontium Budget. *Earth Planet. Sci. Lett.* 211, 173-187.

De La Rocha, C. L. and DePaolo, D. J., 2000. Isotopic Evidence for Variations in the Marine Calcium Cycle over the Cenozoic. *Science* 289, 1176-1178.

Delaney, M. L., Linn, L. J., and Davies, P. J., 1996. Trace and minor element ratios in Halimeda aragonite from the Great Barrier Reef. *Coral Reefs* 15, 181-189.

Elderfield, H. and Gieskes, J. M., 1982. Sr Isotopes in Interstitial Waters of Marine Sediments from deep-sea Drilling Project Cores. *Nature* 300, 493-497.

Fairbanks, R.F., 1989. A 17,000-year glacio-eustatic sea level record: influence of glacial melting rates on the Younger Dryas event and deep-ocean circulation. Nature, 342, 637-642.

Farkaŝ, J., Buhl, D., Blenkinsop, J., and Veizer, J., 2007. Evolution of the Oceanic Calcium Cycle During the late Mesozoic: Evidence from Delta $\delta^{44/40}$Ca of Marine Skeletal Carbonates. *Earth Planet. Sci. Lett.* 253, 96-111.

Faure, G. and Felder, R. P., 1981. Isotopic Composition of Strontium and Sulfur in Secondary Gypsum Crystals, Brown Hills, Transantarctic Mountains. *Journal of Geochemical Exploration* 14, 265-270.

Fietzke, J. and Eisenhauer, A., 2006. Determination of Temperature-Dependent Stable Strontium Isotope ($^{88}$Sr/$^{86}$Sr) Fractionation via Bracketing Standard MC-ICP-MS. *Geochem. Geophys. Geosyst.* 7(8) doi: 10.1029/2006GC001244.

Gaillardet, J., Dupre, B., and Allègre, C. J., 1999. Geochemistry of Large River Suspended Sediments: Silicate Weathering or Recycling Tracer? *Geochim. Cosmochim. Acta* 63, 4037-4051.

Gallup, C. D., Olson, D. M., Edwards, R. L., Gruhn, L. M., Winter, A., and Taylor, F. W., 2006. Sr/Ca-Sea Surface Temperature Calibration in the Branching Caribbean Coral Acropora Palmata. *Geophys. Res. Lett.* 33, 4, L03606, doi:10.1029/2005GL024935.

Godderis, Y. and Veizer, J., 2000. Tectonic Control of Chemical and Isotopic Composition of Ancient Oceans: The Impact of Continental Growth. *Am. J. Sci.* 300, 434-461.

Graham, S. T., Famiglietti, J. S., and Maidment, D. R., 1999. Five-Minute, 1/2 Degrees, and 1 Degrees data sets of Continental Watersheds and River Networks for use in Regional and Global Hydrologic and Climate System Modeling Studies. *Water Resources Research* 35, 583-587.

Haase, K. M., Petersen, S., Koschinsky, A., Seifert, R., Devey, C. W., Keir, R., Lackschewitz, K. S., Melchert, B., Perner, M., Schmale, O., Suling, J., Dubilier, N., Zielinski, F., Fretzdorff, S., Garbe-Schönberg, D., Westernstroer, U., German, C. R., Shank, T. M., Yoerger, D., Giere, O., Kuever, J., Marbler, H., Mawick, J., Mertens, C., Stober, U., Ostertag-Henning, C., Paulick, H., Peters, M., Strauss, H., Sander, S., Stecher, J., Warmuth, M., and Weber, S., 2007. Young Volcanism and Related Hydrothermal Activity at 5° S on the Slow-Spreading Southern Mid-Atlantic Ridge. *Geochem. Geophys. Geosyst.* 8, 17, doi: 10.1029/2006GC001509.

Halicz, L., Segal, I., Fruchter, N., Stein, M., and Lazar, B., 2008. Strontium Stable Isotopes Fractionate in the soil Environments? *Earth Planet. Sci. Lett.* 272, 406-411.

Hubbard, D. K., Miller, A. I., and Scaturo, D., 1990. Production and Cycling of Calcium-Carbonate in a Shelf-edge reef System (St.Croix, United-States Virgin-Islands) - Applications to the Nature of reef Systems in the Fossil Record. *Journal of Sedimentary Petrology* 60, 335-360.

Kisakürek, B., Eisenhauer, A., Böhm, F., Garbe-Schönberg, D., and Erez, J., 2008. Controls on Shell Mg/Ca and Sr/Ca in Cultured Planktonic Foraminifera. *Earth Planet. Sci. Lett* 273, 260-269.

Krabbenhöft, A., Fietzke, J., Eisenhauer, A., Liebetrau, V., Böhm, F., and Vollstaedt, H., 2009. Determination of radiogenic and stable strontium isotope ratios ($^{87}Sr/^{86}Sr/\delta^{88/86}Sr$) by thermal ionization mass spectrometry applying an $^{87}Sr/^{84}Sr$ double spike. *Journal of Analytical Atomic Spectrometry* 24, 1267-1271.

Liebetrau, V., Eisenhauer, A., Krabbenhöft, A., Fietzke, J., Böhm, F., Rüggeberg, A., and Guers, K., 2009. New Perspectives on the Marine Sr-isotope record: $\delta^{88/86}Sr$, $^{87}Sr/^{86}Sr^*$ and $\delta^{44/40}Ca$ Signatures of Aragonitic Molluscs Throughout the last 27 Ma. *Geochim. Cosmochim. Acta* 73, A762.

Lindberg, B. and Mienert, J., 2005. Postglacial Carbonate Production by cold-water Corals on the Norwegian Shelf and their role in the Global Carbonate Budget. *Geology* 33, 537-540.

McArthur, J. M., 1994. Recent Trends in Srontium Isotope Stratigraphy. *Terr. Nova* 6, 331-358.

McArthur, J. M., Howarth, R. J., and Bailey, T. R., 2001. Strontium Isotope Stratigraphy: LOWESS Version 3: Best fit to the Marine Sr-Isotope Curve for 0-509 Ma and Accompanying look-up Table for Deriving Numerical age. *Journal of Geology* 109, 155-170.

Milliman, J. D. and Droxler, A. W., 1996. Neritic and Pelagic Carbonate Sedimentation in the Marine Environment: Ignorance is not Bliss. *Geol. Rundsch.* 85, 496-504.

Mottl, M. J., Wheat, G., Baker, E., Becker, N., Davis, E., Feely, R., Grehan, A., Kadko, D., Lilley, M., Massoth, G., Moyer, C., and Sansone, F., 1998. Warm Springs Discovered on 3.5 Ma Oceanic Crust, Eastern Flank of the Juan de Fuca Ridge. *Geology* 26, 51-54.

Nier , A. O., 1938. The Isotopic Constitution of Strontium, Barium, Bismuth, Thallium and Mercury. *Physical Review* 5, 275-279.

Ohno, T., Komiya, T., Ueno, Y., Hirata, T., and Maruyama, S., 2008. Determination of $^{88}Sr/^{86}Sr$ Mass-Dependent Isotopic and Radiogenic Isotope Variation of $^{87}Sr/^{86}Sr$ in the Neoproterozoic Doushantuo Formation. *Gondwana Res.* 14, 126-133.

Palmer, M. R. and Edmond, J. M., 1989. The Strontium Isotope Budget of the Modern Ocean. *Earth Planet. Sci. Lett.* 92, 11-26.

Palmer, M. R. and Edmond, J. M., 1992. Controls Over the Strontium Isotope Composition of River Water. *Geochim. Cosmochim. Acta* 56, 2099-2111.

Peucker-Ehrenbrink, B. and Miller, M. W., 2004. River Chemistry and Drainage Basin Geology. *Geochim. Cosmochim. Acta* 68, A426-A426.

Ravizza, G., Blusztajn, J., Von Damm, K. L., Bray, A. M., Bach, W., and Hart, S. R., 2001. Sr Isotope Variations in vent Fluids from 9° 46 '- 9° 54 ' N East Pacific Rise: Evidence of a non-zero-Mg Fluid Component. *Geochim. Cosmochim. Acta* 65, 729-739.

Rüggeberg, A., Fietzke, J., Liebetrau, V., Eisenhauer, A., Dullo, W. C., and Freiwald, A., 2008. Stable Strontium Isotopes ($\delta^{88/86}Sr$) in Cold-Water Corals - A new Proxy for Reconstruction of Intermediate Ocean Water Temperatures. *Earth Planet. Sci. Lett.* 269, 569-574.

Schiebel, R., 2002. Planktic Foraminiferal Sedimentation and the Marine Calcite Budget. *Glob. Biogeochem. Cycle* 16, 21.

Stanley, S. M. and Hardie, L. A., 1998. Secular Oscillations in the Carbonate Mineralogy of Reef-Building and Sediment-Producing Organisms Driven by Tectonically Forced Shifts in Seawater Chemistry. *Paleogeogr. Paleoclimatol. Paleoecol.* 144, 3-19.

Stoll, H. M. and Schrag, D. P., 1998. Effects of Quaternary sea Level Cycles on Strontium in Seawater. *Geochim. Cosmochim. Acta* 62, 1107-1118.

Stoll, H. M. and Schrag, D. P., 2000. Coccolith Sr/Ca as a new Indicator of Coccolithophorid Calcification and Growth rate. *Geochem. Geophys. Geosys.* 1, 1999GC000015.

Stoll, H. M., Schrag, D. P., and Clemens, S. C., 1999. Are Seawater Sr/Ca Variations Preserved in Quaternary Foraminifera? *Geochim. Cosmochim. Acta* 63, 3535-3547.

Sun, Y., Sun, M., Lee, T., and Nie, B., 2005. Influence of Seawater Sr Content on Coral Sr/Ca and Sr Thermometry. *Coral Reefs* 24, 23-29.

Vance, D., Teagle, D. A. H., and Foster, G. L., 2009. Variable Quaternary Chemical Weathering Fluxes and Imbalances in Marine Geochemical Budgets. *Nature* 458, 493-496.

Veizer, J., 1989. Strontium Isotopes in Seawater Through time. *Annu. Rev. Earth Planet. Sci.* 17, 141-167.

**Tables:**

**Tab. 1: Sr element and isotope composition of selected rivers**

| Nr. | River | Sample date and location | Sr [mol/a]·$10^8$ | Water discharge [$km^3$/a] | $^{87}Sr/^{86}Sr$ | $^{87}Sr/^{86}Sr^*$ | $^{87}Sr/Sr^{86}_{norm}$ | $\delta^{88/86}Sr$ [‰] |
|---|---|---|---|---|---|---|---|---|
| 1 | Brahmaputra | (06/21/06, 25.2833°N, 89.6333°E) | 3.25 | 510* | 0.719218(26) | 0.719320(3) | 0.709205(3) | 0.317(1) |
| 2 | Danube | (05/04/07, 48.2261°N, 16.4086°E) | 5.71 | 207* | 0.712723(7) | 0.712808(2) | 0.712717(2) | 0.254(4) |
| 3 | Frazer | (08/08/06, 49.5633°N, 121.4028°W) | 0.955 | 112* | 0.718662(1) | 0.718764(6) | 0.718653(6) | 0.31(2) |
| 4 | Ganga | (08/17/07, 24.0553°N, 89.0314°E) | 3.25 | 493* | 0.727702(9) | 0.727798(6) | 0.727705(6) | 0.25(2) |
| 5 | Hudson | (07/02/08, 42.75°N, 73.68°W) | 0.174 | 12** | 0.710328(1) | 0.710425(1) | 0.710332(1) | 0.260(1) |
| 6 | Indus | (02/28/07, 25.4422°N, 68.3164°E) | 3.00 | 90* | 0.711003(24) | 0.711100(4) | 0.710990(4) | 0.31(1) |
| 7 | Lena | n.a. | 5.78 | 525* | 0.709536(20) | 0.709617(9) | 0.709530(8) | 0.243(6) |
| 8 | Mackenzie | (04/07/07, 68.4659°N, 134.1283°W) | 7.30E+08 | 308* | 0.711442(8) | 0.711547(7) | 0.711434(7) | 0.32(2) |
| 9 | Maipo | (01/29/07, -33.6288°N, 70.3548°W) | 1.00 | 3.6*** | n.a. | 0.707506(9) | 0.707355(9) | 0.42(2) |

| | | | | | | | | |
|---|---|---|---|---|---|---|---|---|
| 10 | Sacred Falls Punaluu | n.a. | 1.00 | n.a. | 0.707323(8) | 0.707417(9) | 0.707321(2) | 0.27(3) |
| 11 | Rhine | (8/25/07, 50.9481°N, 6.9714°E) | 4.32 | 69.4* | 0.709377(9) | 0.708799(6) | 0.708713(9) | 0.24(1) |
| 12 | Saint Lawrence | (05/18/08, 45.8586°N, 73.2397°W) | 4.99 | 337* | 0.710362(7) | 0.71048(1) | 0.710354(7) | 0.34(3) |
| 13 | Yangtze | (2007, 30.2872°N, 111.5264°E) | 20.7 | 900** | 0.710587(7) | 0.71072(2) | 0.710587(7) | 0.38(5) |

**Note:** "n.a." = data not available. Data marked with (*) are from (GAILLARDET et al., 1999), (**) (PALMER and EDMOND, 1989) and (***) from the United States Geological Survey (http://www.sage.wisc.edu/riverdata/). The presented errors are given as 2 standard error of the mean ($2\sigma_{mean}$). The $^{87}Sr/^{86}Sr_{norm}$ value is determined from the $\delta^{88/86}Sr$ and the $^{87}Sr/^{86}Sr^*$ value renormalized to $\delta^{88/86}Sr=0$ (see Appendix 2).

**Tab. 2: Sr element ratios and isotope composition of the hydrothermal fluids from MAR, 4°48' S**

| Label | Location | Depth [m] | Fluid [%] | T [°C] | Mg/Sr [mol/mol] | $^{87}Sr/^{86}Sr$* | $\delta^{88/86}Sr$ [‰] |
|---|---|---|---|---|---|---|---|
| 42ROV-3 | 4°48´S, CC | 2990 | 72 | >400 | 303 | 0.707488(4) | 0.361(6) |
| 42ROV-4 | 4°48´S, CC | 2990 | 80 | >400 | 236 | 0.706643(3) | 0.346(5) |
| 42ROV-7 | 4°48´S, CC | 2995 | 88 | >400 | 144 | 0.706276(2) | 0.324(5) |
| 35ROV-8 | 4°48´S, TP | 2990 | 100 | 450 | 3 | 0.705066(3) | 0.26(2) |
| 67ROV-4 | 4°48´S, RL | 3045 | 80 | 366 | 177 | 0.705808(3) | 0.29(1) |
| 67ROV-5 | 4°48´S, RL | 3045 | 98 | 366 | 23 | 0.703857(1) | 0.253(1) |
| 67ROV-6 | 4°48´S, RL | 3045 | 81 | 366 | 164 | 0.705179(1) | 0.294(3) |

**Note:** TP = Turtle Pits, CC = Comfortless Cove; RL = Red Lion. The presented errors are given as 2 standard error of the mean ($2\sigma_{mean}$).

**Tab. 3: Sr burial fluxes and their isotopic composition**

| Carbonate Sediment Type | $CaCO_3$ Deposition [$10^{12}$ mol/a] | $CaCO_3$ polymorph | Mean Sr/Ca [mmol/mol] | Sr Burial Flux ($10^9$ mol/a) | $^{87}Sr/^{86}Sr^*$ | $\delta^{88/86}Sr$ [‰] (SRM987) |
|---|---|---|---|---|---|---|
| | 1. | 2. | 3. | 4. | 5. | 6. |
| Reef Corals (JCp-1 coral standard) | ~6.0 ( 20 %) | Aragonite | ~9.0 | ~54 (31 %) | 0.70923(8) | 0.19(1)‰ |
| *Halimeda* | ~1.5 ( 5 %) | Aragonite | ~11 | ~16 ( 9 %) | 0.70926(3) | 0.27(3)‰ |
| Coccoliths | ~5.0 ( 16 %) | Calcite | 2.2 | ~11 ( 6 %) | 0.70926(3) | 0.26(7)‰ |
| Planktic Foraminifera | ~6.0 ( 20 %) | Calcite | 1.4 | ~8 ( 5 %) | 0.70920(2) | 0.14(1)‰ |
| Continental shelf and slope taxa (mussels, starfish, etc.) | ~13.0 ( 39 %) | Aragonite and calcite | ~6.6 | ~85 (49 %) | 0.70924(1) | 0.22(3)‰ |
| Total Carbonates | ~32.0 (100 %) | --- | n.a. | ~174(100 %) | 0.70926(2) | 0.21(2)‰ |

The values in brackets of columns 5 and 6 correspond to $2\sigma_{mean}$. **Column 4** is calculated from the values of column 1 and 3.
**Column 1: Carbonate deposition rates** are **from** (MILLIMAN and DROXLER, 1996)**.**
**Reef Corals:** values from (HUBBARD et al., 1990). Mean Sr/Ca data are compiled from published data on *Acropora, Diploria, Montastrea, Montipora, Pavona* and *Porites* (COHEN and THORROLD, 2007; GALLUP et al., 2006; SUN et al., 2005). The average ($^{87}Sr/^{86}Sr^*/\delta^{88/86}Sr$)-values are adopted from the longterm average value of the JCp-1 coral standard.
**Halimeda:** Halimeda Sr/Ca ratio is from (DELANEY et al., 1996). The ($\delta^{88/86}Sr/^{87}Sr/^{86}Sr^*$) are measured on Halimeda specimens from Tahiti and the Mediterranean Sea.
**Coccoliths**: the $CaCO_3$ burial rate is from (SCHIEBEL, 2002) and (BROECKER and CLARK, 2009). Mean Sr/Ca ratios are from (STOLL and SCHRAG, 2000). The $\delta^{88/86}Sr$ value is the average of various measurements on laboratory cultured *Emiliania huxleyi* and *Coccolithus pelagicus*.
**Planctic Foraminifera**: the $CaCO_3$ burial rate is from (SCHIEBEL, 2002). Mean Sr/Ca ratios is from (KISAKÜREK et al., 2008). The ($^{87}Sr/^{86}Sr^*/\delta^{88/86}Sr$)-values are determined on *G. ruber* and *G. sacculifer* originating from the core (SO 164-03-4) from the central Caribbean Sea (16°32'37'' N, 72°12'31'' W, 2744 m).
**Continental shelf and slope taxa**: $CaCO_3$ sediments on the continental shelves and slopes are produced by a variety of taxa, including species mentioned above. For further discussion we assume the shelf species to be two-third aragonitic (Sr/Ca ~9 mmol/mol) and one-third calcitic (Sr/Ca ~1.8 mmol/mol) approaching a Sr/Ca ratio of ~6.6 mmol/mol. Note, that the contribution of the shelf taxa is burdened with large uncertainty although they may supply the largest fraction to the Sr burial flux.

**Tab. 4: Sources of Sr to the ocean:**

| Sr Sources | | $^{87}Sr/^{86}Sr$ | $^{87}Sr/^{86}Sr_{norm}$ | $^{87}Sr/^{86}Sr^*$ | $\delta^{88/86}Sr$ [‰] | Flux [$10^9$ mol/yr] |
|---|---|---|---|---|---|---|
| **River discharge** | $J_{River}$ | 0.7119[1] | 0.7113(4) | 0.7114(8) | 0.315(8) | ~33.3[1] |
| **Groundwater discharge** | $J_{GW}$ | 0.7110[2] | n.a | n.a | n.a | ~16.5[2] |
| **Oceanic crust-seawater interaction at mid-ocean ridges** | $J_{HydEnd}$ | 0.7025[3] | 0.70438(3) | 0.7045(5) | 0.27(1) | ~2.3[3] |
| **Low-temperature interaction on ridge flanks and within the cold oceanic crust** | $J_{OCC}$ | 0.7025[3] | n.a. | n.a. | n.a. | ~0.8[3] |
| **Diagenetic reflux from marine sediments** | $J_{DIA}$ | 0.7084[1] | n.a. | n.a. | n.a. | ~3.4[1] |
| **Sr Flux weighted average** | $J_{Input}$ | n.a. | n.a. | ~0.7104(8) | ~0.310(8) | ~56.3 |

**Note**: (1) (PALMER and EDMOND, 1989), (2) (BASU et al., 2001), (3) (DAVIS et al., 2003). All ($^{87}Sr/^{86}Sr^*/\delta^{88/86}Sr$)-values are from this study. The major Sr inputs into the ocean are river discharge ($J_{RW}$), groundwater discharge ($J_{GW}$) and oceanic crust-seawater interaction ($J_{OCH}$) at mid ocean ridges. All other Sr fluxes generated by low temperatures interaction on ridge flanks, ($J_{OCC}$), Sr inputs from buried sedimentary pore waters and from recrystallized sediments ($J_{DIA}$) are considered to be within the statistical uncertainty of the large Sr contributions to the ocean. "n.a.": **n**ot **a**vailable. The Sr isotope composition of the input is calculated from the values above. For simplification and due to the lag of data we assumed that the ($^{87}Sr/^{86}Sr^*/\delta^{88/86}Sr$) -values of $J_{GW}$ is equal to $J_{Rivers}$ and that the ($^{87}Sr/^{86}Sr^*/\delta^{88/86}Sr$)-values of $J_{OCC}$ and of $J_{DIA}$ is equal to $J_{HydEnd}$.

**Figure captions:**

**Fig. 1:** The $(^{87}Sr/^{86}Sr^*/\delta^{88/86}Sr)_{River}$-values are plotted in a three isotope plot. It can be seen that there is a considerable scatter in both the $^{87}Sr/^{86}Sr^*$ and the $\delta^{88/86}Sr$ values. The Sr flux weighted average mean of all rivers is marked by a square.

**Fig. 2**: $(^{87}Sr/^{86}Sr^*/\delta^{88/86}Sr)$-values of hydrothermal fluid samples. Assuming that the pure hydrothermal solution is free of Mg (Mg/Sr=0) hydrothermal $\delta^{88/86}Sr$ (a) and $^{87}Sr/^{86}Sr^*$ (b) end members can be extrapolated (dotted line) from our data. Circles refer to Comfortless Cove (CC) and Turtle Pits (TP), whereas triangles refer to the Red Lion (RL) hydrothermal field from the mid-Atlantic Ridge.

**Fig. 3:** Three isotope plot showing the flux weighted average Sr isotope values of rivers, hydrothermal fluids, marine carbonates and seawater. The seawater value and the carbonate value form a mass-dependent fractionation line whereas the river and the hydrothermal values form a binary mixing line. The calculated Sr isotope composition of the joint riverine and hydrothermal input value plot along the binary mixing line but is considerably offset from the isotope composition of the marine carbonate (output) and the intercept value. Note, the calculated glacial input value is close to the carbonates.

**Figures:**

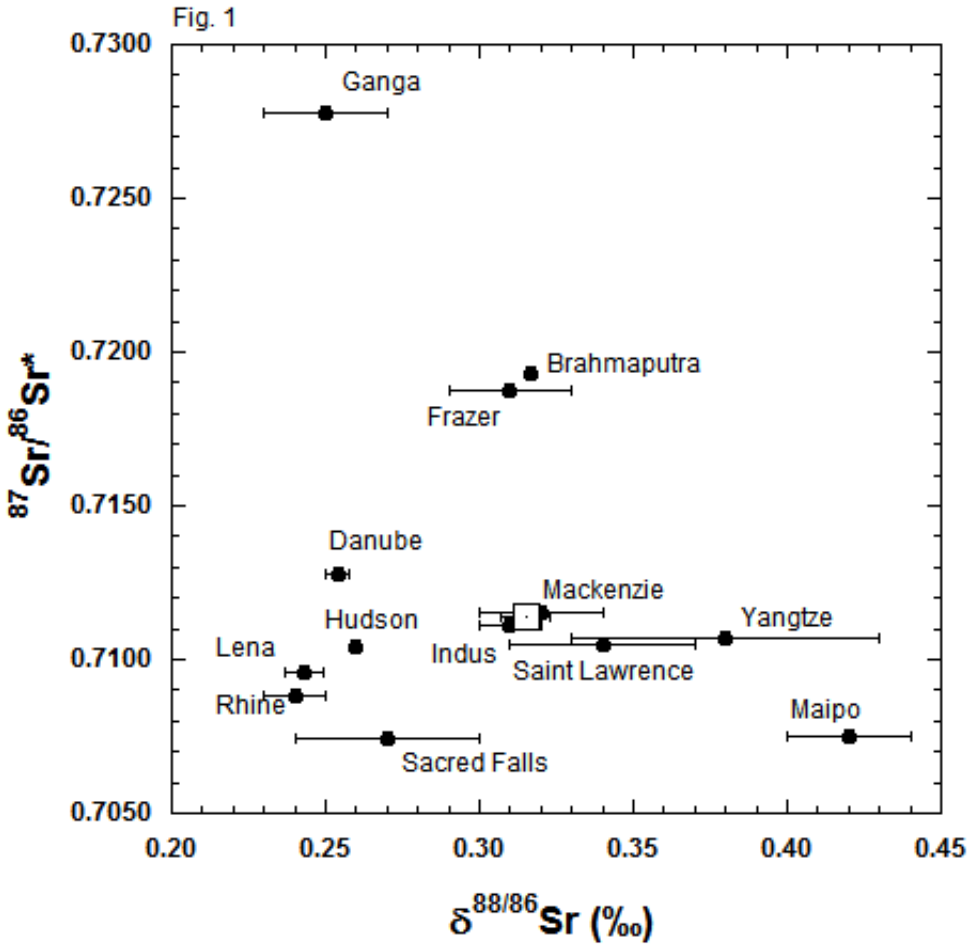
Fig. 1
0.7300
0.7250
0.7200
0.7150
0.7100
0.7050
0.20
0.25
0.30
0.35
0.40
0.45
$^{87}Sr/^{86}Sr^*$
$\delta^{88/86}Sr$ (‰)
Ganga
Brahmaputra
Frazer
Danube
Mackenzie
Hudson
Yangtze
Lena
Indus
Saint Lawrence
Rhine
Maipo
Sacred Falls

Fig. 2

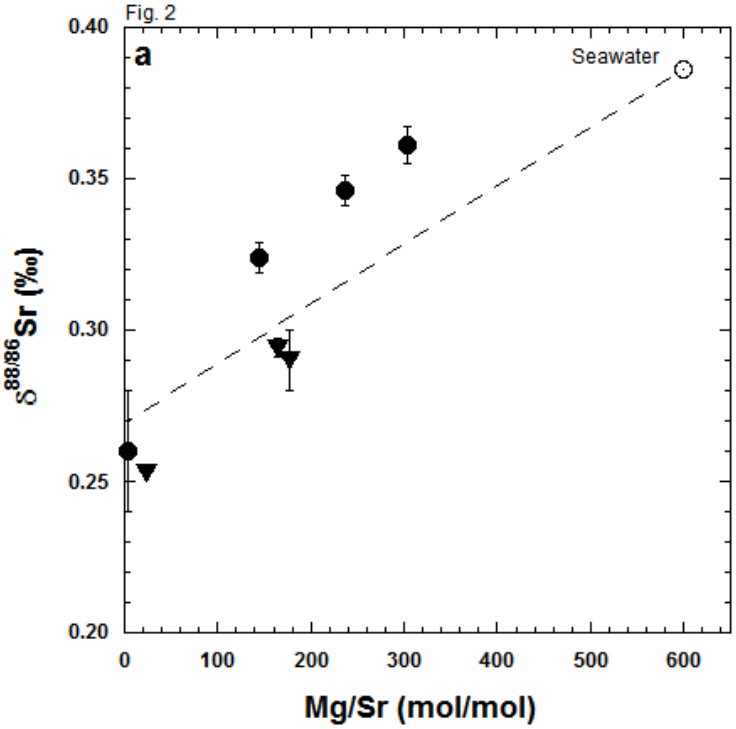
a
Seawater
0.40
0.35
0.30
0.25
0.20
0
100
200
300
400
500
600
δ88/86Sr (‰)
Mg/Sr (mol/mol)

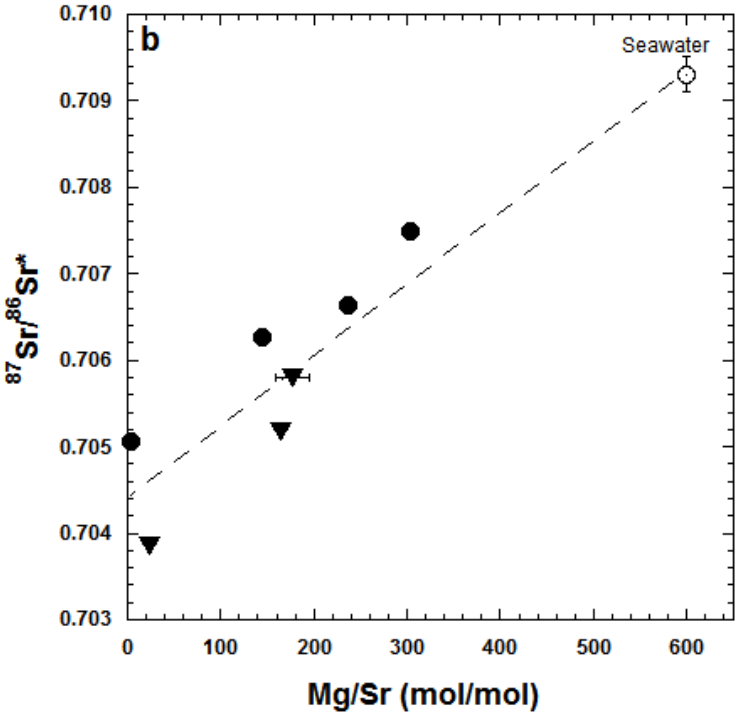
b
Seawater
0.710
0.709
0.708
0.707
0.706
0.705
0.704
0.703
$^{87}Sr/^{86}Sr^*$
0
100
200
300
400
500
600
Mg/Sr (mol/mol)

Fig. 3

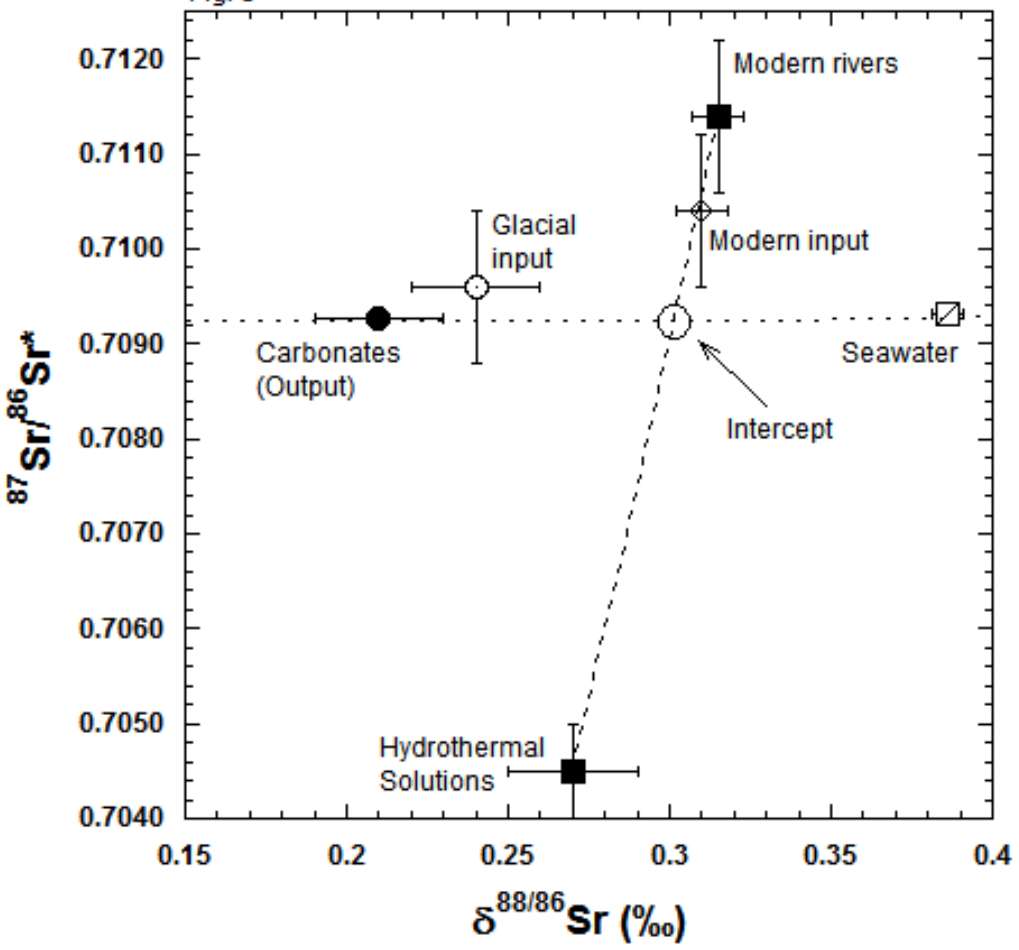
Modern rivers
Modern input
Glacial input
Carbonates (Output)
Seawater
Intercept
Hydrothermal Solutions
0.7120
0.7110
0.7100
0.7090
0.7080
0.7070
0.7060
0.7050
0.7040
0.15
0.2
0.25
0.3
0.35
0.4
87Sr/86Sr*
δ88/86Sr (‰)

**Appendix:**

## 1. Notation

The term ($^{87}Sr/^{86}Sr^*/\delta^{88/86}Sr$) refers to paired naturally fractionated $^{87}Sr/^{86}Sr$ and $^{88}Sr/^{86}Sr$ ratios. In order to distinguish between this ratio and the normalized ($^{87}Sr/^{86}Sr_{Norm}/\delta^{88/86}Sr=0$) one ($^{87}Sr/^{86}Sr_{Norm}$) we marked the $^{87}Sr/^{86}Sr$ ratio determined with the Sr double spike technique with a "*" ($^{87}Sr/^{86}Sr^*$). Note, the difference between $^{87}Sr/^{86}Sr^*$ and $^{87}Sr/^{86}Sr_{Norm}$ reflects mass-dependent isotope fractionation.

## 2. Sr mass fractionation

$^{87}Sr/^{86}Sr^*$ and $^{88}Sr/^{86}Sr$ are determined from a double spike measurement following the procedure as previously published by (KRABBENHÖFT et al., 2009). The relationship between the traditional radiogenic $^{87}Sr/^{86}Sr$ ratio ($^{87}Sr/^{86}Sr_{Norm}$) and $^{87}Sr/^{86}Sr^*$ is defined by equation A1:

$$A1: \quad \frac{\left(\frac{^{87}Sr}{^{88}Sr}\right)_{Norm}}{\left(\frac{^{87}Sr}{^{88}Sr}\right)^{*}} = \left[\frac{\left(\frac{^{88}Sr}{^{86}Sr}\right)_{Nier}}{\left(\frac{^{88}Sr}{^{86}Sr}\right)^{*}}\right]^{\frac{\ln(m_{87}/m_{86})}{\ln(m_{88}/m_{86})}}$$

The $(^{87}Sr/^{86}Sr)_{Nier}$ value was once defined by (NIER 1938) to be 8.375209 corresponding to a $\delta^{88/86}Sr=0$ relative to NIST SRM 987. The masses for the various Sr isotopes are: $m_{86}$ = 85.909273 $m_{87}$ =86.908890, and $m_{88}$ = 87.905625. For more details see (KRABBENHÖFT et al., 2009).

## 3. Error notation and propagation

All presented statistical uncertainties represent 2 standard errors of the mean ($2\sigma_{Mean}$). We present the statistical uncertainties for $^{87}Sr/^{86}Sr$ and $\delta^{88/86}Sr$ in brackets. The values in the brackets refer to the last digit of the measured values. For example $^{87}Sr/^{86}Sr$ = 0.711111(1) correspond to 0.711111±0.000001 and $\delta^{88/86}Sr$=0.386(1) correspond to 0.386±0.001 ‰.

## 4. Isotope equilibrium

Following the approach of (DE LA ROCHA and DEPAOLO, 2000) the isotope conditions during equilibrium concerning elemental ocean´s input and output can be mathematically described for the Sr isotope systems as follows. Note, the equations are given for $\delta^{88/86}Sr$, but are analog for $^{87}Sr/^{86}Sr^*$, too:

$$A2: \quad N_{Sr} \cdot \frac{\partial \delta^{\frac{88}{86}}Sr_{Seawater}[\text{‰}]}{\partial t} = J_{Input} \cdot \left( \delta^{\frac{88}{86}}Sr_{Input}[\text{‰}] - \delta^{\frac{88}{86}}Sr_{Seawater}[\text{‰}] \right) - J_{Output} \cdot \Delta_{Output}$$

$$A3: \quad \Delta_{Output} = \delta^{\frac{88}{86}}Sr_{Carbonates}[\text{‰}] - \delta^{\frac{88}{86}}Sr_{Seawater}[\text{‰}]$$

In a steady-state ocean where both the Sr isotope composition of the ocean and the amount of Sr present in the ocean is not changing anymore ($d[Sr]_{Seawater}/dt = d(\delta^{88/86}Sr(t))/dt = 0$) equation A2 and A3 are reduced to A4:

$$\delta^{\frac{88}{86}}Sr_{Input}[\text{‰}] = \delta^{\frac{88}{86}}Sr_{Output}[\text{‰}]$$